Towards nanostructures membranes for the artificial kidney

Master of Science Degree in Chemical Engineering

Madalena Lopes,[1] Mónica Faria[1], Vasco D.B. Bonifácio[2,3]

[1]CeFEMA, and Departamento de Engenharia Química, Instituto Superior Técnico, Universidade de Lisboa, Campus Alameda, 1049-001 Lisboa, Portugal, e-mail: madalena.b.lopes@tecnico.ulisboa.pt.
[2]Departamento de Bioengenharia, Instituto Superior Técnico, Universidade de Lisboa, Campus Alameda, 1049-001 Lisboa, Portugal.
[3]iBB-Institute for Bioengineering and Biosciences and iH4B-Institute for Health and Bioeconomy, Instituto Superior Técnico, Universidade de Lisboa, Campus Alameda, 1049-001 Lisboa, Portugal.

1. Introduction

Chronic kidney disease (CKD) has a prevalence from 11 to 13% in the world's population and the main treatment to replicate some of the kidney's functions is hemodialysis (HD)[1]. During each HD session, blood is drawn from the patient via an access device (e.g. fistula, graft, catheter) and is passed through an extracorporeal circuit where it is processed and then returned to the patient. The main component of the extracorporeal circuit is the hemodialyzer also known as the artificial kidney (AK) which is composed of semi-permeable membranes that remove accumulated toxins and excess water while retaining vital blood components such as blood cells, platelets, and proteins. While blood flows in one direction, dialysate, flows in counter current direction. The dialysate is a solution of pure water, electrolytes, and salts such as bicarbonate, sodium and potassium, that transports the waste compounds removed from the blood. Also, it maintains the eletrolyte balance in patients' blood and enhances the solute removal through diffusion.

The European Uremic Toxin Work Group (EUTox) is a research team which focuses essentially on identifying solute retention and removal in CKD patients, and on the deleterious impact of uremic toxins (UTs) on biological systems[2]. The EUTox team developed an interactive database that classifies UTs in three main groups: small water-soluble compounds, middle molecules, and protein-bound compounds (Table 1).

Table 1: Classification of uremic toxins proposed by EUTox

Group	MW range	Protypes	MW (Da)
Small water-soluble compounds	< 500 Da	Urea	60
		Creatinine	113
		Uric Acid	168
Middle molecules	500 – 60000 Da	β_2-Microglobulin	11818
Protein bound compounds	< 500 Da	*p*-Cresyl Sulfate	31
		Indoxyl Sulfate	212

One of the biggest challenges of HD is the removal of the protein bound uremic toxin's (PBUT's) which, in blood, are bond to albumin forming very large structures that cannot permeate through the hemodialyzer membranes.

PBUT's such as indoxyl sulfate (IS) and *p*-cresyl sulfate (pCS) are known to cause cardiovascular complications by inducing inflammatory responses or by causing endothelial or other vascular dysfunctions[3,4]. Hence, several studies focus on improving the removal of these toxins. A clinical study[5] has shown that certain pharmaceutical drugs, such as ibuprofen (IBF) and furosemide (FUR), bind more strongly to albumin than specific PBUT's, and that, by injecting large amounts of ibuprofen into the blood circulation of patients prior to undergoing HD, the removal of IS and pCS was enhanced. However, long-term administration of high doses of these drugs is unsustainable for the patient's health.

The main objective of this work is to use Human Serum Albumin (HSA) binding competitors to enhance PBUT removal without drug administration. The strategy relies on IBF incorporation of in the HD membrane, taking advantage of its high binding affinity to HSA (2.7×10^6 M^{-1})[6]. Figure 1 depicts the main innovation undertaken in this work.

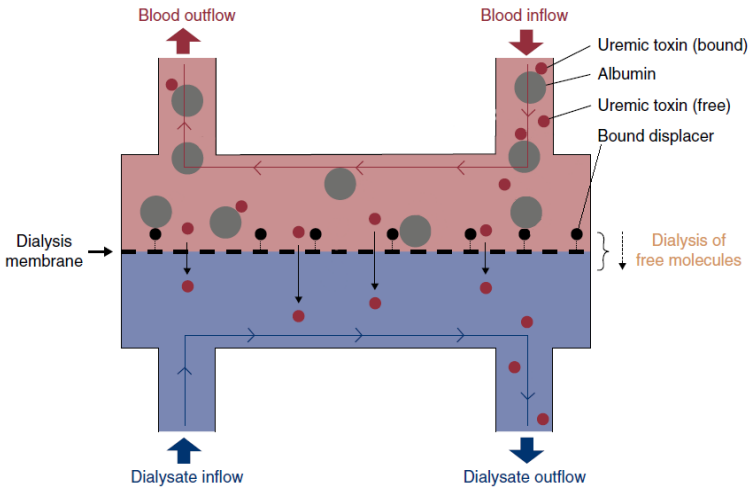

Figure 1: Displacer concept proposed in this thesis.

The HD membranes chosen for this work are monophasic hybrid cellulose acetate/silica (SiO_2) membranes. Incorporation of silica is made by coupling phase inversion and sol-gel technologies through silica precursors which reacts with hydroxyl groups present in cellulose acetate. The monophasic hybrid membranes have integral asymmetric cross section structures characterized by a very thin dense active layer and a much thicker and porous. The thin dense layer is responsible for the membrane selectivity and presents the highest resistance to permeation while the porous substructure confers mainly mechanical resistance to the membrane.

2. Materials and Methods

2.1. Materials

Membranes were synthesized with cellulose acetate, with around 40% of acetylation degree, from Sigma-Aldrich (CA; (MW~30000 g/mol, ≥ 97%), tetraethyl orthosilicate (TEOS, 98%), purchased from Alfa Aesar, (3-(triethoxysilyl)–propylamine (APTES, ≥98%) purchased from Sigma-Aldrich, formamide (≥99.5%) purchased from Carlo Erba, acetone (≥99.6%) purchased from Labsolve, and nitric acid purchased from LabSolve. Permeation experiments were carried out with urea purchased from Merck, creatinine purchased from Sigma- Aldrich, uric acid purchased from Alfa Aesar and bovine serum

albumin (BSA) purchased from Sigma-Aldrich. The quantification of BSA was carried out according to the Bradford protein assay. The molecular weight cut-off (MWCO) was determined using polyethylene glycol (PEG) standards: PEG 400 and PEG 2000 purchased from Sigma-Aldrich, PEG 3000, PEG 6000, PEG 10000 and PEG 35000 purchased from Merck and Dextran T40 and T70 purchased from Amersham Pharmacia BioTech AB.

2.2. Precursors Synthesis

2.2.1. PURE$_{G4}$ dendrimer derivatives

The main goal of this work was the incorporation of IBF in the active layer of the membranes with potential use in HD. A first approach aimed the synthesis of IBF precursors for physical incorporation in the membranes, using dendrimers, producing mixed matrix membranes. Four compounds were synthesized by two methods: i) incorporation of IBF in a polyurea dendrimer (IBF@PURE$_{G4}$ and IBF-PURE$_{G4}$) and ii) incorporation of a dye in PURE$_{G4}$, rose bengal (RB) and methyl red (MR), in replacement of IBF, to have a visual proof of the physical incorporation (RB-PURE$_{G4}$ and MR-PURE$_{G4}$). IBF@PURE$_{G4}$ is the encapsulation of IBF in the core of the PURE$_{G4}$ dendrimer, with a IBF loading capacity up to 50 wt%[7]. IBF-PURE$_{G4}$ is the conjugation of IBF into PURE$_{G4}$ surface, prepared following the literature[8]. RB-PURE$_{G4}$ and MR-PURE$_{G4}$ followed the same synthetic protocol of IBF-PURE$_{G4}$. All the four precursors were successfully synthesized, as confirmed by Nuclear Magnetic Ressonance (NMR).

2.2.2. Silyl derivatives

A second approach aimed IBF conjugation to the membrane matrix via the silica precursors used in the membrane synthesis, already proven to be incorporated in the polymer matrix[9]. Three compounds were synthesized, two of them conjugated to IBF using TEOS and APTES silica precursors, and other conjugated to the MR dye using APTES. The IBF-TEOS reaction followed a literature protocol[10] and the resulting product was found to be a TEOS disubstituted precursor having two IBF molecules (Figure 2). The IBF-TEOS structure was confirmed by NMR and mass spectrometry.

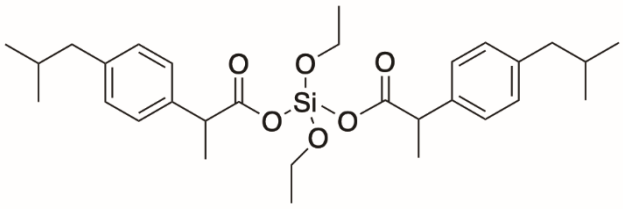

Figure 2: Chemical structure of the disubstitued precursor IBF-TEOS.

The APTES precursors synthesis followed a reported protocol,[11] resulting in target IBF-APTES and MR-APTES, where IBF and MR are conjugated to APTES via the amine group.

2.3. Membranes Fabrication

Four monophasic hybrid membranes were fabricated by coupling sol-gel[12] and phase inversion[13–15] technologies: CA95-SiO_2-$(CH_2)_3NH_2$, as a reference for monophasic hybrid membranes; CA95-SiO_2-$(CH_2)_3NH_2$-MR, as a visual proof of the precursor incorporation (MR-APTES); CA90-SiO_2-$(CH_2)_3NH_2$-IBF and CA95-IBF-SiO_2-$(CH_2)_3NH_2$, the competitive binding membranes with IBF

precursors, IBF-APTES and IBF-TEOS, respectively. One mixed matrix membrane (MMMs) was fabricated by the physical incorporation designated as CA99-RB-PURE$_{G4}$. For comparison purposes, a pure polymer, CA100, membrane was also synthesized. All monophasic hybrid membranes were synthesized with a SiO_2/NH_2 molar ratio of 80:20 (Table 2). The membranes are fabricated in batches, and one batch can produce up to 2 membranes sheets with 675 cm^2 (B) or 4 membranes sheets with 420 cm^2 (S).

Table 2: Composition of the casting solutions, wt% of CA and precursors and solvent evaporation time for the CA100, CA95-SiO_2-$(CH_2)_3NH_2$, CA95-SiO_2-$(CH_2)_3NH_2$-MR, CA90-SiO_2-$(CH_2)_3NH_2$-IBF, CA99-RB-PURE$_{G4}$ and CA95-IBF-SiO_2-$(CH_2)_3NH_2$ membranes.

	Quantity (g)					
	CA100	**CA95-SiO_2-$(CH_2)_3NH_2$**	**CA95-SiO_2-$(CH_2)_3NH_2$-MR**	**CA90-SiO_2-$(CH_2)_3NH_2$-IBF**	**CA99-RB-PURE$_{G4}$**	**CA95-IBF-SiO_2-$(CH_2)_3NH_2$**
CA	4.25	4.10	4.10	3.95	4.25	4.10
Formamide	7.50	7.25	7.25	6.98	7.50	7.25
Acetone	13.25	12.78	12.78	12.30	13.25	12.78
TEOS	-	0.60	0.60	1.20	-	-
APTES	-	0.16	-	-	-	0.16
HNO_3	-	3 drops	3 drops	3 drops	-	3 drops
Synthesized precursor	-	-	MR-APTES	IBF-APTES	RB-PURE$_{G4}$	IBF-TEOS
	-	-	0.16	0.32	0.18	0.60
CA (wt%)	100	95	95	90	99*	95
Total SiO_2 (wt%)	0	5	5	10	0	5
No. sheets**	2(B)	2(B)	4(S)	2(B)	4(S)	4(B)***
Solvent evap. time	30s	30s	30s	30s (1st sheet) 15s (2nd sheet)	30s	**** 15s (1st sheet) 30s (2nd sheet)

*1wt% is from RB-PURE$_{G4}$; **(B) is for big sheets with 675 cm^2 and (S) for small sheets with 420 cm^2; ***two batches, each one produced two membrane sheets; **** sheets from second batch.

The casting solution of the monophasic hybrid membranes was prepared in two steps. First, CA, formamide and acetone were mixed in a reaction vessel to allow the complete dissolution of CA. After 5 h of mixing, TEOS and APTES and nitric acid were added to the mixture, promoting hydrolysis and hetero-condensation during the casting solution homogenization step. The final solution was placed under stirring for another 19 h, resulting in a total homogenization time of 24 h for CA. The casting solution for the mixed matrix membrane, CA99-RB-PURE$_{G4}$, is similar to the casting solution of the monophasic hybrid membrane but, instead of adding TEOS, APTES and nitric acid, functionalized PURE$_{G4}$ is added after the 5 h of mixing. A reference casting solution of the pure CA100 membrane was prepared by mixing CA, formamide and acetone for 24 h. All the membranes casting solutions were cast

on glass plates with a 250 µm Gardner knife at room temperature and a specific solvent evaporation time was performed for each membrane sheet, after which they were quenched in a cooling bath containing water at 4 ºC. After a residence time of approximately 1 h in the coagulation bath, the membranes were detached from the glass plate and stored separately in deionized water at 4 ºC.

2.4. Membranes Characterization

2.4.1. Experimental set-up

The laboratory experimental set-up used for the permeation studies is detailed in

Figure 3 and has been previously described[16]. The single hemodialysis membrane module (SHDMM) is where the membrane is placed and is a five-part unit. The thickness of these units provides transport only by convection and not by diffusion. Some parameters are collected from the installation that are very important for further characterization and monitoring experiments of the membranes. Transmembrane pressure (TMP) (1) is calculated as average pressures in blood compartment minus average pressure in the dialysate compartment. Rejection factor (2) is a percentage of how much solute, initially in feed solution, after a certain time, passes through the membrane to the permeate in a steady state condition. The pressure drop (ΔP) (3) is the difference of pressures from blood compartment inlet and outlet from the membrane module. The microchannel height (4) from SHDMM compartments is an important indicator of membrane fouling. Shear stress (τ) (5) is the frictional force exerted by blood flow on the vessel wall and is very important avoid blood damaging as platelet activation and hemolysis.

$$TMP = \frac{P_{S1} + P_{S2}}{2} - P_{S3} \quad (1)$$

$$f_{rejection} = 1 - \frac{\bar{C}_{permeate,t}}{\bar{C}_{feed,0}} \quad (2)$$

$$\Delta P = P_{S1} - P_{S2} \quad (3)$$

$$2B = 2 * \sqrt[3]{\frac{Q_F * \mu * L}{\Delta P * W} * \frac{3}{2}} \quad (4)$$

$$\tau\,[Pa] = \frac{3 * \mu * Q_F}{2 * W * B^2} = \frac{B * \Delta P}{L} \quad (5)$$

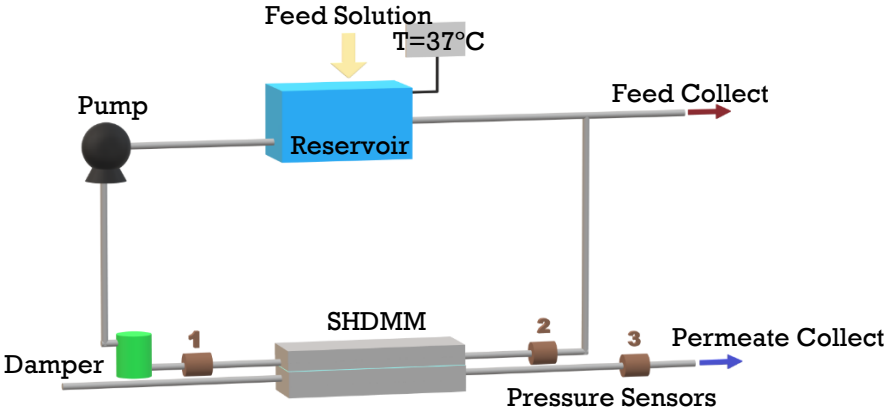

Figure 3: Laboratory setup for permeation studies.

2.4.2. Permeation studies

To evaluate the mass transfer properties associated to the metabolic functions of the kidney several parameters must be studied, namely, the hydraulic permeability (Lp), MWCO, rejection coefficient to small water soluble UTs, and long-term BSA filtration.

2.4.2.1. Hydraulic Permeability

The permeability experiments were performed using deionized water at 37 ºC. Permeate was collected over 120 seconds, weighed, and transformed in volume by water density at 37 ºC (ρ= 0,993 g mL^{-1}). A plot of permeate flux *versus* TMP passing through the origin gives a straight line which the resulting slope yield hydraulic permeability of the membrane. These values were obtained in triplicate for each feed flow rate (from 28.4 to 214.2 mL min^{-1}) and TMP values from and 10 to 150 mmHg.

2.4.2.2. Molecular weight cut-off

The MWCO of a membrane refers to the lowest *molecular weight* solute (in Daltons) in which 90% of the solute is retained by the membrane. In this study, six PEGs with increasing MW: 3000, 6000, 10000, 20000 and 35000 Da and dextrans T40 and T70 with MW of 40000 and 70000 Da, respectively, were used. Quantification was achieved with a Total Organic Carbon (TOC) analyzer (TOC-V CSH from Shimadzu). The TOC analyzer reports the concentration of organic carbon in the sample analyzed. Calibration curves were made for all polymers. Before starting the experiments, the SHDMM is washed for approximately 30 minutes with ultrapure MiliQ water. The initial solution of each polymer was prepared with a concentration of 600 mg L^{-1} and is placed in reservoir at 37 ºC and recirculated for 10 minutes. The priming volume was estimated at 40 mL and, to avoid dilution, this volume was collected in feed before starting the assay. Permeate and feed samples are collected at 0, 10, 50 and 90 minutes and the concentration of the polymer in the permeate was considered zero at time zero.

2.4.2.3. Rejection coefficient to small water-soluble UTs

The quantification of each toxin was obtained by spectrophotometry. Each toxin has a maximum absorption band and calibration curves were obtained for each one using a UV-visible spectrophotometer (UV-1700 PharmaSpec from Shimadzu) using deionized water as the blank. Creatinine, urea and uric acid were used and detected at a wavelength of 230, 200 and 293 nm, respectively with initial feed solutions concentrations of 240 mg L^{-1}, 4,6 g L^{-1} and 60 mg L^{-1}, respectively, with refers to pathological values for CKD patients.[17,18] These experiments were performed as described in section 2.4.2.2. Deionized water was used instead of MiliQ water. Feed and permeate samples were collected at 15 minutes time intervals for a total of 90 minutes. Concentrations were calculated using the calibration curve performed for the three UTs, and the rejection factor was calculated using equation (2).

2.4.2.4. Long-term BSA filtration

A solution of BSA with a concentration of 900 mg L^{-1} was prepared. During the first 90 minutes, samples from feed and permeate streams were collected at intervals of 15 minutes, and after that, at intervals of 30 minutes until a total of 8 hours of filtration was achieved. The detection was made by UV spectrophotometry. Concentrations higher than 100 mg L^{-1} have a linear behavior at 595 nm[19]. For lower

concentrations (<100 mg L^{-1}), linearization is made with the ratio for 590 and 450 nm[20]. BSA concentrations were determined using the calibration curves, as described[19,20].

3. Results and discussion

Table 3 shows the permeation parameters evaluated for the different membranes fabricated.

Table 3: Permeation experiments results done for each membrane synthesized.

Membrane	Description			Characterization			
		Lp (mL $h^{-1}m^{-2}$ $mmHg^{-1}$)	MWCO (kDa)	Urea rejection (%)	creatinine rejection (%)	uric acid rejection (%)	BSA rejection (%)
CA100	• Pure CA membrane	50.3	19	4.3	9.9	0.0	99.6
CA99-$PURE_{G4}$-RB	• Mixed matrix membrane containing pure CA and $PURE_{G4}$ dendrimer • Pink membrane, dye conjugated to $PURE_{G4}$ dendrimer	*	*	*	*	*	*
CA95-SiO_2-$(CH_2)_3NH_2$	• Monophasic hybrid membrane	89.4	27	6.5	5.8	4.2	99.3
CA95-SiO_2-$(CH_2)_3NH_2$-MR	• Monophasic hybrid membrane • Orange membrane, dye conjugate to APTES	92.4	*	*	*	*	*
CA90-SiO_2-$(CH_2)_3NH_2$-IBF(1): first sheet	• Competitive binding monophasic hybrid membrane • IBF conjugated to APTES (IBF-APTES)	48.1	*	*	**	0.0	93.6
CA90-SiO_2-$(CH_2)_3NH_2$-IBF(2): second sheet	• Competitive binding monophasic hybrid membrane • IBF conjugated to APTES (IBF-APTES)	16.9	*	*	*	*	*
CA95-IBF-SiO_2-$(CH_2)_3NH_2$(1).1: 1^{st} sheet, 1^{st} batch	• Competitive binding monophasic hybrid membrane • IBF conjugated to TEOS (IBF-TEOS) • Solvent evaporation 30s	14-0	*	*	*	*	*
CA95-IBF-SiO_2-$(CH_2)_3NH_2$(2).1: 2^{nd} sheet, 1^{st} batch	• Competitive binding monophasic hybrid membrane • IBF conjugated to TEOS (IBF-TEOS)	41,4	*	*	*	*	*
CA95-IBF-SiO_2-$(CH_2)_3NH_2$(1).2: 1^{st} sheet, 2^{nd} batch	• Competitive binding monophasic hybrid membrane	*	*	*	*	*	*

	• IBF conjugated to TEOS (IBF-TEOS) • IBF-TEOS improved solubilization in casting solution						
CA95-IBF-SiO_2-$(CH_2)_3NH_2$(2).2: 2nd sheet, 2nd batch	• Competitive binding monophasic hybrid membrane • IBF conjugated to TEOS (IBF-TEOS) • IBF-TEOS improved solubilization in casting solution	27,4	62,5	*	*	4,4	89,5

*not performed; **inconclusive experiment.

3.1. IBF precursors and membrane fabrication

3.1.1. Control membranes

Figure 4 show photos of CA99-RB-PURE$_{G4}$ and CA95-SiO_2-$(CH_2)_3NH_2$-MR membranes. The pink coloration (Figure 4, left) confirms the physical incorporation of RB-PURE$_{G4}$ in the CA matrix. Permeation performance was not performed due to time constrains. The membrane with MR-APTES, CA95-SiO_2-$(CH_2)_3NH_2$-MR, showing orange coloration (Figure 4, right) corroborates the conjugation of MR-APTES in the CA matrix.

Figure 4: CA99-RB-PURE$_{G4}$ pink membrane (left) and CA95-SiO_2-$(CH_2)_3NH_2$-MR orange membrane (right).

3.1.2. Silyl derivatives

For the silica precursors, the differences between TEOS/APTES and the newly synthesized precursors rely on steric constrains introduced by IBF conjugation. IBF-TEOS has only two available ethoxy groups for further reaction (sol-gel), and the IBF is three times bigger. in IBF-APTES, IBF is bonded to the APTES terminal amine. And, in sol-gel[12], the hydrolysis rate is decreased by substituents that increase steric crowding around silicon which is what happens in these compounds. Thereupon, from this point of view, IBF-APTES possess a lower steric hindrance and should suffer higher hydrolysis. Both precursors have pros and cons, but both are expected to conjugate with the available hydroxyl groups in CA.

3.2. Permeation studies

3.2.1. Hydraulic Permeability

The most obvious result Is that the Lp of the dyed monophasic hybrid CA95-SiO_2-$(CH_2)_3NH_2$-MR (control) membrane is much higher than all the other membranes. This may be because MR-APTES had residual impurities, resulting from the synthetic step, as shown in the NMR spectrum. These contaminants may interfered in the membrane structure, thus explaining the Lp results. The second obvious result is that the competitive binding CA90-SiO_2-$(CH_2)_3NH_2$-IBF membrane shows two different results for Lp which could be justified by the discrepancies in the synthesis method (different solvent evaporation time).

3.2.2. MWCO

The MWCO was estimated to be 27 kDa for the CA95-SiO_2-$(CH_2)_3NH_2$ membrane, 19 kDa for the CA100 membrane and 62.5 kDa for CA95-IBF-SiO_2-$(CH_2)_3NH_2$(2).2. With the understanding that all membranes reject solutes with MWs greater than 20 kDa, it was predicted that vital blood components such as albumin, platelets, and blood cells would be rejected by the membranes. Furthermore, it is envisioned that molecules belonging to two different classes of uremic toxins proposed by EUTox - small water-soluble compounds and middle molecules - can be removed, as they are able to cross the membrane.

3.2.3. Rejection coefficient to small water-soluble UTs

The rejection coefficient towards creatinine, uric acid and urea for the CA100 membrane were 4.3%, 0.0% and 9.9%, respectively; and for CA95-SiO_2-$(CH_2)_3NH_2$ membrane, 6.5%, 4.2% and 5.8%, respectively. These results are in agreement with what was discussed before in terms of MWCO, given that urea (60 Da), creatinine (113 Da), and uric acid (168 Da) have much lower MW than the CA95-SiO_2-$(CH_2)_3NH_2$ and CA100 membranes' MWCO. In competitive binding membranes, CA90-SiO_2-$(CH_2)_3NH_2$-IBF(1) and CA95-IBF-SiO_2-$(CH_2)_3NH_2$(2).2, a residual leaching was observed, which was proven to be IBF-APTES and IBF-TEOS, respectively. This leaching tends to diminish with time, however, interferes with detection of creatinine and urea in UV-visible spectophotometer making uric acid assay the only experiment reliable for these membranes. Rejection coefficients of 0.0% and 4.4% for CA90-SiO_2-$(CH_2)_3NH_2$-IBF(1) and CA95-IBF-SiO_2-$(CH_2)_3NH_2$(2).2 membranes were achieved.

3.2.4. BSA filtration

The BSA permeation experiments were carried out for over 8 h with initial concentration of 900 mg L^{-1} of BSA giving rejection coefficients to BSA for CA100, CA95-SiO_2-$(CH_2)_3NH_2$, CA90-SiO_2-$(CH_2)_3NH_2$-IBF(1) and CA95-IBF-SiO_2-$(CH_2)_3NH_2$(2).2 membranes of 99.4%, 99.2%, 93.6% and 89.5%, respectively. The decreasing values throughout the membranes are concordant to the enlargement of pore sizes shown by MWCO results. TMP and microchannel heights values stayed constant through all the 8 h assay evidencing the absence of compound deposition and membrane fouling.

4. Conclusions

The integral asymmetric, hybrid monophasic cellulose acetate/silica and mixed matrix membranes were characterized and incorporated with novel compounds to enhance PBUT's removal. $PURE_{G4}$ dendrimer was functionalized with IBF and two different dyes, rose bengal (RB) and methyl red (MR) aiming membrane nanostructuration and IBF functionalization, or visual proof of conjugation in the case of the dyes. Silica precursors were conjugated with IBF or MR, for IBF membrane incorporation or visual proof of conjugation in the case of MR. The structure and purity of intermediates were confirmed by NMR and/or mass spectrometry. Membranes with MR and RB, CA99-RB-$PURE_{G4}$ and CA95-SiO_2-$(CH_2)_3NH_2$-MR, stayed colored after the experiments proving an efficient incorporation into the CA polymer matrix. Membranes with 5% and 10% silica content showed similar permeation properties. Hydraulic permeabilities were lower than pristine CA membrane, probably due to IBF steric hindrance and hydrophobicity. Rejection factors for uric acid were low, thus evidencing efficient removal of small water-soluble molecules. Determined MWCO showed a significantly increase in pore size, which led to lower BSA rejection.

5. References

1. Hill NR, Fatoba ST, Oke JL, et al. *PLoS One*. 2016;11(7):1-18.
2. Vanholder R, Abou-Deif O, Argiles A, et al. *Semin Dial*. 2009;22(4):323-328.
3. Glorieux G, Vanholder R. *Hemodiafiltration - A New Era*. 2010;168:117-128.
4. Faria M, de Pinho MN. *Transl Res*. Published online 2020:1-20.
5. Tao X, Thijssen S, Kotanko P, et al. *Sci Rep*. 2016;6(December 2015):2-10.
6. Maheshwari V, Tao X, Thijssen S, Kotanko P. *Toxins (Basel)*. 2021;13(9).
7. Restani RB, Silva AS, Pires RF, et al. N *Part Part Syst Charact*. 2016;33(11):851-858.
8. Mota P, Pires RF, Serpa J, Bonifácio VDB. *Molecules*. 2019;24(17):2-9.
9. Mendes G, Faria M, Carvalho A, Gonçalves MC, de Pinho MN. *Carbohydr Polym*. 2018;189:342-351.
10. Tacke R, Burschka C, Richter I, Wagner B, Willeke R.. *J Am Chem Soc*. 2000;122(35):8480-8485.
11. Rastegar AJ, Vosgueritchian M, Doll JC, Mallon JR, Pruitt BL. *Langmuir*. 2013;29(23):7118-7124.
12. Guglielmi M. *Mater Chem Phys*. 1990;26(2):211-212.
13. Kunst B, Sourirajan S. *J Appl Polym Sci*. 1974;18(11):3423-3434.
14. Pageau L, Sourirajan S. *J Appl Polym Sci*. 1972;16(12):3185-3206.
15. Loeb S, Sourirjan S. *Sea Water Demineralization by Means of an Osmotic Membrane*. ; 1963:117-132.
16. Janeca A, Rodrigues FSC, Gonçalves MC, Faria M. *Membranes (Basel)*. 2021;11(11):825.
17. Duranton F, Cohen G, De Smet R, et al. *J Am Soc Nephrol*. 2012;23(7):1258-1270.
18. Vanholder R, Smet R De, Glorieux G, Argilés A. *Kidney Int*. 2003;63:1934-1943.
19. Bradford MM. *Anal Biochem*. 1976;(72):248-254.
20. Zor T, Selinger Z. *Anal Biochem*. 1996;236(2):302-308.